Prominent Higher-Order Contributions to Electronic Recombination

C. Beilmann,[1] P. H. Mokler,[1] S. Bernitt,[1] C. H. Keitel,[1] J. Ullrich,[1] J. R. Crespo López-Urrutia,[1] and Z. Harman[1,2]

[1]*Max-Planck-Institut für Kernphysik, Saupfercheckweg 1, 69117 Heidelberg, Germany*

[2]*ExtreMe Matter Institute (EMMI), Planckstraße 1, 64291 Darmstadt, Germany*

(Received 24 May 2011; published 29 September 2011)

Intershell higher-order (HO) electronic recombination is reported for highly charged Ar, Fe, and Kr ions, where simultaneous excitation of one K-shell electron and one or two additional L-shell electrons occurs upon resonant capture of a free electron. For the mid-Z region, HO resonance strengths grow unexpectedly strong with decreasing atomic number Z ($\propto Z^{-4}$), such that, for Ar ions the 2nd-order overwhelms the 1st-order resonant recombination considerably. The experimental findings are confirmed by multiconfiguration Dirac-Fock calculations including hitherto neglected excitation pathways.

DOI: 10.1103/PhysRevLett.107.143201 PACS numbers: 34.80.Lx, 31.30.jc, 32.80.Hd, 52.25.Os

Electron-electron interactions not only strongly affect the electronic energy levels of atoms and ions, but also the reaction dynamics of these systems. Indeed, very effective resonant photorecombination mechanisms are observed in stellar as well as Earth-bound plasmas [1,2]. Here, Auger decay (cf. e.g., [3]) and its time reversal, dielectronic recombination (DR) (see, e.g., [4,5]) play a prominent role. Usually, theory uses independent-particle models to treat them, where only two electrons interact and all others are assumed to be merely spectators. Higher-order (HO) interactions between more than two electrons, and especially those in different shells—intershell processes—are often considered as negligible.

In this Letter we show, both experimentally and theoretically, the importance of hitherto unrecognized HO contributions in *intershell* electron-electron interaction by using electronic recombination as indicator. In earlier work 2nd-order resonant (dubbed trielectronic) recombination was reported for interactions within one electronic shell (*intrashell*) [6], and its importance was established for Be-like systems, where both $2s$ electrons are coevally excited inside their ground state shell [7,8]. In the present work, we deal with HO intershell resonant recombination, where a K-shell electron interacts during recombination simultaneously with one or more additional L-shell electrons. We have already reported faint contributions of such processes in highly charged Kr ions [9], but beyond that, no genuine higher-order intershell photorecombination results have been published thus far. Nonetheless, in the experiment described in [10], a triply excited state was formed by trielectronic electron capture in Li^+ ions ($Li^+(1s^2) + e \rightarrow [Li(2s^2 2p)]^{***}$) and only doubly ionizing decay (to $Li^{2+}(1s)$), but no radiative stabilization of neutral Li—essential for a complete recombination—was observed. Other experiments utilizing channeling techniques achieved just upper limits for intershell HO recombination [11].

In intershell processes with a core excitation, the high energy and momentum transfer would suggest a strong preponderance of the 1st-order contribution. We question this common assumption by experimentally comparing the 1st-order DR process, in this case K-LL, to the corresponding 2nd-order trielectronic (TR, e.g., KL-LLL) and 3rd-order quadruelectronic (QR, e.g., KLL-$LLLL$) recombination, as shown in Fig. 1. We apply the standard Auger notation and extend it in an analogous manner.

Resonant electronic recombination for ions A^{q+} of charge $q+$, can generally be represented by $A^{q+} + e \rightarrow [A^{(q-1)+}]^{(n+1)*} \rightarrow A^{(q-1)+} + \Sigma_i h\nu_i$, where n is the order of the recombination process nR with $n = 1$, 2, and 3 for DR, TR, and QR, respectively. Multiply [up to $(n+1)$ times] excited intermediate states denoted by $[A^{(q-1)+}]^{(n+1)*}$ may stabilize radiatively, thus completing the process of recombination. The number of emitted photons depends on the decay pathways, being typically $\leq n+1$ (neglecting possible cascades). HO recombination processes, nR with $n > 1$, can only occur through configuration mixing, i.e., via correlations between the electrons in the intermediate state, $|nR\rangle = \Sigma_k c_k |\alpha_k JP\rangle$, where c_k is the mixing coefficient for the configuration state function $|\alpha_k JP\rangle$ and α_k contains all the quantum numbers to define the configuration state function. Our calculations employ multiconfiguration Dirac-Fock (MCDF) bound-state wave functions with configuration mixing, and include correlation effects

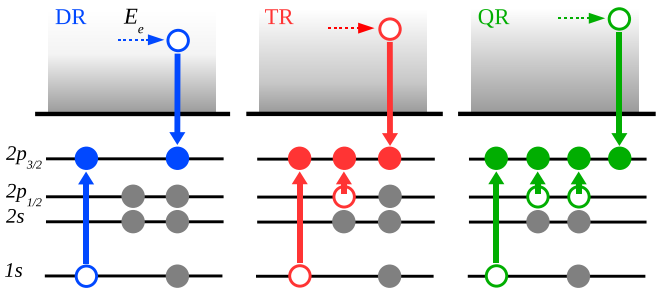

FIG. 1 (color online). Diagrams for K-L intershell resonant recombination of 1st, 2nd, and 3rd order—dielectronic (DR), trielectronic (TR), and quadruelectronic (QR) recombination [blue (left), red (middle), and green (right)], respectively.

to all orders [9,12] with coding similar to [13] (see also [14]).

The experiments were performed at the Heidelberg electron beam ion traps (EBITs) [15,16]. Highly charged ions (HCI) of Ar, Fe, and Kr produced by continuous electron impact were evaporatively cooled within the trap [17]. By scanning the electron beam energy E_e across the resonances, ions recombine efficiently. Product ions in multiply excited states, $|nR\rangle$, can relax to the ground state by x-ray emission monitored by means of an x-ray detector. Plotting the characteristic K_α x-ray intensity against E_e yields the respective resonance energies. Figure 2 shows a spectrum for Fe ions and electrons around 5 keV. Strong cooling is a prerequisite for the achieved full-width-at-half-maximum of roughly 7 eV [17], since hot ions would interact in a broader spatial region with less well defined electrostatic potential, i.e. collision energies, E_e.

The spectrum in Fig. 2 comprises resonances for Li-like to O-like Fe ions. Calculated positions and strengths of the resonances are also indicated, with the charge state distribution empirically adjusted. Therefore, only relative resonance strengths within each single isoelectronic sequence (IS) can be compared. Moreover, the electron beam energies were calibrated using two well-known He-like DR resonances. Good agreement between experiment and calculations is observed for all charge states. We clearly identify 2nd-order recombination resonances, TR, in B-like, C-like, and N-like ions. No TR resonances are found for Be-like ions, and indeed, due to parity rules they are strongly suppressed in this IS [9]. For C-like ions even the 3rd-order recombination, QR, is observed as a faint but detectable feature around 4975 eV (superimposed also by a QR contribution from Be-like ions).

The 2nd-order contributions are already rather strong for C-like Fe ions: the overall TR/DR strengths ratio is about 0.5. The comparison of Kr, Fe, and Ar for this IS in Fig. 3 demonstrates the strong increase in the ratio TR/DR with decreasing atomic number Z. The energy scales for the different ions are normalized by Z^2, i.e., approximately to the binding energy. Resonances of the low-Z species are less separated since the fine structure splitting $\propto Z^4$. The experimental resolution is similar in all spectra shown. For the C-like species DR and TR contributions (as well as that for QR in Fe) are indicated using the color code of Fig. 1. The region highlighted in Fig. 3 is marked for C-like Fe at the bottom in Fig. 2.

The TR/DR strengths ratio for C-like ions as a function of Z is depicted in Fig. 4; see left-side ordinate. The experimental ratios extracted from the spectra (Fig. 3) are very well predicted. The increase in the TR/DR ratio is striking: For Ar the 2nd-order exceeds the 1st-order strength by a factor of 1.4. The observed behavior will become more prevalent at even lower Z: Already for C-like Mg ions, TR is expected to contribute more than twice to the total recombination as compared to DR. For neighboring ion species, B- and N-like IS, similar dependencies can be stated.

In order to elucidate the unexpected magnitude and strong Z dependence of TR in comparison to DR, first we estimate the probability of electron capture leading to a multiply-excited state, i.e., the perturbative factor $\langle \mathrm{TR}|\sum r_{ij}^{-1}|\mathrm{DR}\rangle/(E_{\mathrm{TR}} - E_{\mathrm{DR}})$ describing the ratio of TR to DR amplitudes. At low Z, it may approach unity since

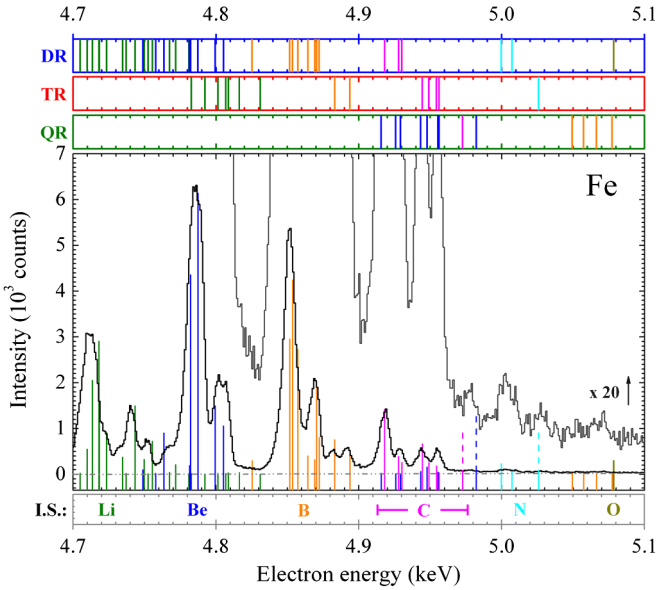

FIG. 2 (color online). Experimental photorecombination spectrum of Fe ions for Li-like to O-like species compared to our MCDF calculations. Top: resonance energies for the different recombination orders. Bottom: IS color coded for this spectrum. The region of C-like resonances is indicated.

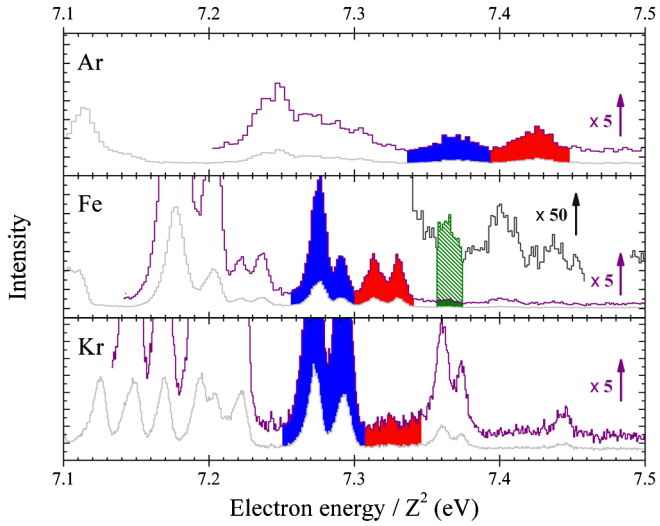

FIG. 3 (color online). Comparison of the C-like recombination lines for Ar, Fe and Kr ions. DR, TR and partially QR lines are marked by blue, red and green colors, respectively. The energy scale of the spectra is normalized by Z^2.

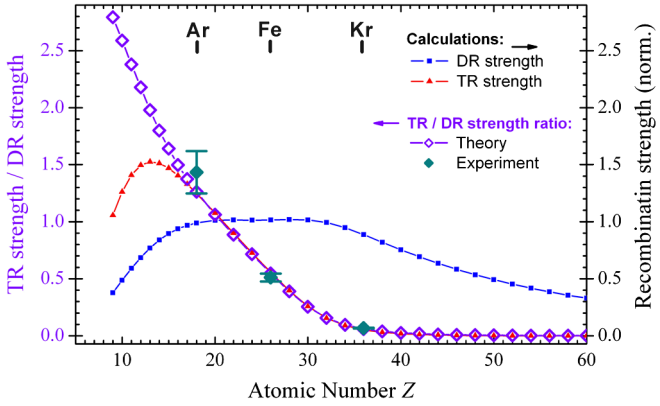

FIG. 4 (color online). Ratio of TR to DR resonance strengths for C-like ions versus atomic number Z, comparison between experiment and theory—left-side ordinate. Additionally, the calculated DR and TR resonance strengths normalized to the maximum of the DR strengths are shown (right-side ordinate).

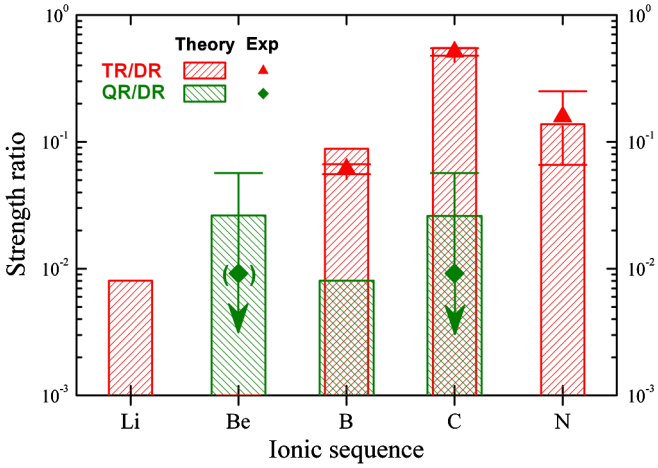

FIG. 5 (color online). Ratio of HO strengths to the 1st-order ones for Fe ions. Red color for the TR/DR ratio (theory: red bars; exp.: red triangles) and green color for the QR/DR ratio (theory: green bars; exp.: green diamonds).

the Coulomb operator acts on the strongly overlapping $|\mathrm{TR}\rangle$ and $|\mathrm{DR}\rangle$ autoionizing state functions, yielding a transition matrix element (numerator) of a few eVs, while the $(E_{\mathrm{TR}} - E_{\mathrm{DR}})$ splitting (denominator) is also in that range. Therefore, we treat the DR-TR mixing nonperturbatively.

Now, the total radiative width of the TR state can be larger at low Z than that of the DR one. This second contribution finally makes TR stronger than DR. We consider the general Z-dependence of the Auger rates (A_a)—nonrelativistically with Z^0—and the radiative ones (A_r)—with Z^4 (see, e.g., [2] or the overview in [18]; for the relativistic dependences of the Auger rates see [13]). Starting from the time inverted process, the autoionization (Auger process), and applying the principle of detailed balance, the strength for DR $(\propto E_e^{-1} A_a \Sigma A_r / (\Sigma A_a + \Sigma A_r))$ can be parametrized by (see, e.g., [19])

$$S_{\mathrm{DR}} \approx [b_1 Z^{-2} + c_1 Z^2]^{-1}, \tag{1}$$

where b_1 and c_1 refer to the Auger and radiative decay channels, respectively. From this we expect for the high-Z region which is dominated by large radiative rates a $1/Z^2$ dependence of the DR strength, for the low-Z region dominated by the Auger rates a Z^2 increase, and in the mid-Z region relative Z independent DR strengths. Our calculations reproduce this behavior, see DR strengths given in Fig. 4—right-side ordinate.

Also for the HO processes the principle of detailed balance can be used to evaluate the recombination strengths. The main difference there is hidden in the individual production rates for the intermediate recombination states. As an additional interaction of an electron is involved these HO Auger rates depend on Z. Compared to the central Coulomb force the electron-electron interaction will decrease with $1/Z$; therefore, unlike the dielectronic capture rates displaying a Z^0 dependence, the trielectronic capture rates (squared matrix elements) will show a $1/Z^2$ behavior yielding a general Z dependence of the TR strengths of

$$S_{\mathrm{TR}} \approx [a_2 Z^{-2} + b_2 + c_2 Z^4]^{-1}, \tag{2}$$

where a_2 refers to the decay channel for the HO Auger process, b_2 and c_2 to the 1st-order Auger and radiative decay channels, respectively. The result of our dedicated MCDF calculations of the TR strength is shown in Fig. 4, too cf. right-side axis. It can be approximated reasonably well by the given parametrization [Eq. (2)]. The maximum of the TR strength is shifted toward lower Z values around Mg and decreases beyond that on the high-Z side with a high power ($\propto Z^{-4}$).

As the total DR strength is about constant in the mid Z range ($17 \lesssim Z \lesssim 34$) due to the interplay between Auger and radiative rates (cf. also [19]), the Z dependence of the ratio gives us directly the absolute Z behavior of the TR resonance strength. Only below $Z = 15$ where the TR strength starts to turn over toward the maximum the ratio increases further as shown by the calculations in Fig. 4 (left-side ordinate). Predictions and experiment agree well.

The surprisingly strong increase in HO recombination strength for low-Z ions is a result of the interplay of the Auger and radiative rates and the Z dependence of the mixing parameters for the states involved in the HO channels. However, on the basis of the considerations given above, this behavior can be understood.

In Fig. 5 the TR and QR strengths are compared for Fe with the corresponding DR ones for the different IS from Li- to N-like. Note that 2nd-order *KL-LLL* TR processes are only possible for certain occupancy levels of the L shell, namely, for Li- to N-like species. For Be-like ions, no TR was found, since parity rules strongly suppress this channel. For the 3rd-order QR, occupancy restrictions makes *KLL-LLLL* only possible for Be- to C-like ions.

The results from our calculations give again good agreement with the experiment. Disregarding the anomaly for Be-like ions caused by parity rules, the TR contributions increase with the number of available electrons up to C-like ions indicating the increase in correlations. The relative QR resonance strength is exceptionally large for Be-like systems, as the TR channels are closed. For N-like ions the relative TR strength is diminished due to the reduced number of final channels. The experimental values given for QR have large uncertainties caused by the blend of Be-like and C-like QR resonances and by the faintness of the detected feature, which is assigned equally to the two ionic species, according to our calculations. For the Be-like ions additional QR contributions may be hidden under the C-like recombination lines; cf. Fig. 2.

In summary, we find prominent HO contributions for *K-L intershell* resonant electronic recombination which increase considerably with decreasing atomic number Z. This is a result of the Z^{-2} dependence of the 2nd-order Auger decay rate. Moreover, the increase of the number and strength of radiative decay channels for the multiply-excited intermediate state contributes to this behavior. For the lightest C-like ions TR overwhelms the 1st-order DR process by more than a factor of 2. These processes populate multiply-excited states decaying to the ground state through photon emission. Therefore, they result in a removal of energetic electrons from, and thus in cooling of, the plasma containing the species of interest. Since an excitation of a K-shell electron is involved, the amount of energy converted from kinetic, i. e. thermal, into radiation is by roughly 2 orders of magnitude larger in each recombination step than that seen in *intrashell* TR processes [5,6] at low kinetic energies.

This work illustrates the predominance of correlation effects at lower Z. It is interesting to note that the HO effects are so prominent in such intershell processes with large momentum and energy transfers. Including them in radiative-collisional plasma codes should enhance their predictive power, since the plasma state should be measurably affected. Spectroscopic diagnostics might be sensitive to x-ray satellite transitions populated through TR. Both facts could lead to a misinterpretation of temperatures and density of magnetically confined Earth-bound and also of astrophysical plasmas.

The HO processes in photorecombination can be used to test in a defined way and with a controlled number of active partners models describing collective electron reactions as, e. g., in shake-up or shake-off processes [20], which have also been found in recent experiments with high-power attosecond lasers [21]. Alternatively, 2nd- and 3rd-order processes investigated here may be viewed in terms of two-step 1 and two-step 2 models discussed for ionization processes [22]. These channels are included in our all-order calculations. Here, pathways aiming beyond independent-particle models are indicated by inclusion of one, or even two, additional correlations in interactions of HCI core and electrons. The experimental control of the number of bound electrons at different Z, as demonstrated here, allows one to test theories aiming at developing fully ''collective'' reaction models. This is another manifestation of a broader set of phenomena related to multielectron resonant behavior. Very recent examples are resonances occurring due to the presence of neighboring atoms or ions in molecules or clusters [23,24] or even in dense plasmas [25], where HO collisional resonances also have to be taken into account.

The work of Z. H. was supported by the Alliance Program of the Helmholtz Association (HA216/EMMI).

[1] H. S. W. Massey and D. R. Bates, Rep. Prog. Phys. **9**, 62 (1942).
[2] A. Burgess, Astrophys. J. **139**, 776 (1964).
[3] T. Åberg and G. Howat, in *Corpuscles and Radiation in Matter I*, edited by S. Flügge, Encyclopedia of Physics (Springer-Verlag, Berlin, 1982).
[4] D. A. Knapp *et al.*, Phys. Rev. A **47**, 2039 (1993).
[5] S. Schippers, J. Phys. Conf. Ser. **163**, 012001 (2009).
[6] M. Schnell *et al.*, Phys. Rev. Lett. **91**, 043001 (2003).
[7] S. Schippers *et al.*, International Review of Atomic and Molecular Physics (IRAMP) **1**, No. 2, 109 (2010).
[8] I. Orban *et al.*, Astrophys. J. **721**, 1603 (2010).
[9] C. Beilmann *et al.*, Phys. Rev. A **80**, 050702(R) (2009).
[10] A. Müller *et al.*, Phys. Rev. Lett. **63**, 758 (1989).
[11] M. Chevallier *et al.*, Phys. Rev. A **61**, 022724 (2000).
[12] Z. Harman *et al.*, Phys. Rev. A **73**, 052711 (2006).
[13] P. Zimmerer, N. Grün, and W. Scheid, J. Phys. B **24**, 2633 (1991).
[14] K. G. Dyall *et al.*, Comput. Phys. Commun. **55**, 425 (1989).
[15] J. R. Crespo López-Urrutia *et al.*, Phys. Scr. **T80**, 502 (1999).
[16] S. W. Epp *et al.*, Phys. Rev. Lett. **98**, 183001 (2007).
[17] C. Beilmann *et al.*, JINST **5**, C09002 (2010).
[18] P. H. Mokler and F. Folkmann, in *Structure and Collisions of Ions and Atoms*, edited by I. A. Sellin, Topics in Current Physics Vol. 5 (Springer-Verlag, Berlin, 1978), p. 201.
[19] A. P. Kavanagh *et al.*, Phys. Rev. A **81**, 022712 (2010).
[20] H. Aksela, A. Aksela, and N. Kabachnik, in *VUV and Soft X-Ray Photoionization*, edited by U. Becker and D. Shirley, Physics of Atoms and Molecules (Plenum, New York, 1996), p. 401.
[21] M. Uiberacker *et al.*, Nature (London) **446**, 627 (2007).
[22] J. McGuire, *Electron Correlation Dynamics in Atomic Collision, no. 8 in Cambridge Monographs on Atomic, Molecular and Chemical Physics* (Cambridge University Press, Cambridge, England, 1997).
[23] R. Santra *et al.*, Phys. Rev. Lett. **85**, 4490 (2000).
[24] N. Sisourat *et al.*, Nature Phys. **6**, 508 (2010).
[25] C. Müller *et al.*, Phys. Rev. Lett. **104**, 233202 (2010).